α-Tocopherol-induced radical scavenging activity in carbon nanotubes for thermo-oxidation resistant ultra-high molecular weight polyethylene-based nanocomposites

N.Tz. Dintcheva [a,*], R. Arrigo [a], C. Gambarotti [b], S. Carroccio [c], G. Filippone [d], F. Cicogna [e], M. Guenzi [b]

[a] Dipartimento di Ingegneria Civile, Ambientale, Aerospaziale, dei Materiali, Università di Palermo, Viale delle Scienze, Ed. 6, 90128 Palermo, Italy
[b] Dipartimento di Chimica, Materiali ed Ingegneria Chimica "G. Natta", Politecnico di Milano, Piazza L. da Vinci 32, 20133 Milano, Italy
[c] Consiglio Nazionale delle Ricerche – ICTP UOS Catania, Via P. Gaifami 18, 95126 Catania, Italy
[d] Dipartimento di Ingegneria Chimica, dei Materiali e della Produzione Industriale (INSTM Consortium – UdR Naples), Università di Napoli Federico II, Piazzale V. Tecchio 80, 80125 Napoli, Italy
[e] Consiglio Nazionale delle Ricerche CNR – ICCOM UOS Pisa, Area della Ricerca, Via G. Moruzzi 1, 56124 Pisa, Italy

Received 16 October 2013
Accepted 25 February 2014
Available online 3 March 2014

1. Introduction

The unusual mechanical, electrical and magnetic properties of carbon nanotubes (CNTs) have motivated a flurry of interest in exploiting their applications for advanced nanocomposite materials, especially polymer-based nanocomposites. Adding CNTs to a polymer matrix can improve mechanical properties and/or provide new functionalities,

---

[*] *Corresponding author:* Fax: +39 09123860841.
E-mail address: nadka.dintcheva@unipa.it (N.Tz. Dintcheva).

e.g. electrical conductivity and magnetic properties [1,2]. Unfortunately, CNTs exhibit a marked tendency to agglomerate and/or aggregate, forming stable bundles that make difficult their homogeneous and uniform dispersion within the matrix [3,4]. An effective strategy to improve the dispersibility of CNTs in polymer matrices is their surface functionalization and/or modification. Numerous approaches are reported in literature, such as (i) defect functionalization [5], (iii) covalent [6] and (iii) non-covalent [7] functionalization, and (iv) functionalization through click chemistry [8]. Among others, physical immobilization is a quite simple non-covalent functionalization approach that allows the immobilization and transport of functional molecules devoid of suitable functional groups to be covalently bonded to CNT surface.

α-Tocopherol, hereafter referred to as "VE" being one of the forms of vitamin E, is a natural molecule able to react with the free radicals in the cell membranes and protect polyunsaturated fatty acids from oxidative degradation. The pronounced antioxidant activity of tocopherol is due to the extraction of the hydrogen atom from the –OH group onto the aromatic ring, with formation of tocopheroxyl radicals able to react with free peroxidic radical. VE can be profitably used as antioxidant and stabilizer for polymeric matrices such as polyolefins [9,10] and bio-polyesters [11]. Moreover, VE has been employed in recent years to increase the bi-stability and bio-compatibility of polymeric materials, e.g. for the stabilization of ultra-high molecular weight polyethylene (UHMWPE) components used in joint arthroplasty [12–14]. The rationale for using VE is improving the oxidation resistance and enhancing the fatigue strength and wear resistance of cross-linked UHMWPE.

Immobilizing VE onto CNTs could lead up to a promising class of multifunctional fillers, able to reinforce and stabilize at the same time a host polymer. In addition, the immobilization of the antioxidant molecules could prevent their loss by volatilization, migration or extraction during either processing or long-term service. In this work VE–functionalized multi-walled CNTs (CNTs/VE) have been prepared by physically immobilization of VE molecules on the outer surface of CNTs bearing covalently-linked carboxylic acid and long-chain alkyl ester groups. Then, UHMWPE-based nanocomposites have been prepared by hot compaction, and their thermo-oxidation resistance has been investigated through rheological analyses and infrared spectroscopy. The samples show thermo-oxidation resistance much higher than what expected on the basis of the inherent antioxidant activity of the VE. Such a surprising result is believed to be due to the specific interaction between the CNTs and the VE molecules. Two plausible chemical mechanisms are proposed to explain the formation of structural defects on CNT surface. The latter represent acceptor-like localized states, being ultimately responsible for the achieved excellent antioxidant feature.

2. Experimental part

2.1. Materials

The UHMWPE is a commercial grade purchased by Sigma–Aldrich. It has weight-average molecular weight 3–6 MDa, softening point $T = 136\ ^\circ C$ (Vicat, ASTM D 1525B), melting point $T_m = 138\ ^\circ C$ (determinate by DSC) and density 0.94 g/mL at 25 °C.

Commercial grade (Cheap Tubes, USA) multi-walled CNTs bearing covalently linked –COOH groups (CNTs-COOH, –COOH content about 1 wt.%) have been used. The main properties are: outer diameter OD = 150–200 nm, inner diameter ID = 10–20 nm, length L = 10–20 μm, purity >95 wt.%, ash <1.5 wt.%, specific surface area SSA > 60 m^2/g and electrical conductivity EC > 10^{-2} S/cm. Bare multi-walled CNTs (Cheap Tubes, USA) were used as reference. They have OD = 150–200 nm, ID = 10–20 nm, L = 10–20 μm, purity >95 wt.%, ash <1.5 wt.%, SSA > 40 m^2/g and EC > 10^{-2} S/cm.

1-Octadecanol, *N,N′*-dicyclohexylcarbodiimide (DCC) and (±)-α-tocopherol, a natural anti-oxidant molecule coming from vegetable oil, all supplied by Sigma–Aldrich, were used as received. The VE has molecular weight 430.71 g/mol.

2.2. CNT functionalization

2.2.1. Esterification of the CNTs-COOH to obtain alkyl-f-CNTs

The CNTs-COOH were subjected to chemical modification to obtain CNTs functionalised with long chain alkyl ester groups (alkyl-*f*-CNTs) considering the chemical protocol sketched in Fig. 1. First, 0.500 g of CNTs-COOH (1) were added to the solution of 1-octadecanol, (0.250 g, 0.93 mmol) and DCC, (0.100 g, 0.49 mmol) in dry 40 mL of tetrahydrofuran (THF). The resulting suspension was then sonicated in a 2 Lt ultrasonic bath (power 260 W) for 1 min and left under vigorous stirring at room temperature for 4 days. After that, the black suspension was filtered, the solid was washed 5 times with hot dimethylformamide (DMF) and 5 times with hot methanol, and it was finally dried at 80 °C overnight.

2.2.2. Immobilization/adsorption of VE molecules onto CNTs-COOH and alkyl-f-CNTs surface

The VE molecules were immobilized/adsorbed on the outer surface of the CNTs follow: 0.200 g of either CNTs-COOH or alkyl-*f*-CNTs were added to a solution of α-tocopherol (0.100 g, 0.23 mmol) in 10 mL of THF. The resulting suspension was sonicated in a 2 Lt ultrasonic bath (power 260 W) for 30 min and filtered over a glass Buchner funnel. The black solid was finally dried at 80 °C for 5 h.

2.3. Nanocomposite preparation

The UHMWPE powder and 1 wt.% of CNTs were manually mixed at room temperature until a homogeneous black powder was obtained. The blends were then hot compacted at 210 °C for 5 min and under a pressure of 1500 psi to get thin films (thickness less than 100 μm) for the subsequent analyses. The pure UHMWPE and UHMWPE/VE were subjected to the same procedure for comparison.

2.4. Characterizations

A Fourier Transform Infrared Spectrometer (FT-IR) (Spectrum One FT-IRspectrometer, Perkin Elmer) was used to record the infrared spectra. Transmission FT-IR analyses of the various

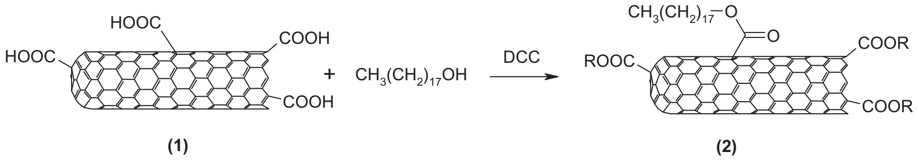

Fig. 1 – Esterification of CNTs-COOH (1) to alkyl-*f*-CNTs (2).

kinds of CNTs were performed aiming at assessing the actual immobilization of the VE molecules. The spectra were acquired from potassium bromide (KBr) pellets prepared by mixing dry KBr with 1 wt.% of CNTs in a mortar and pressing the resulting powder at 200 bar. Three different batches per sample were tested, collecting 32 scans between 4000 and 500 cm^{-1} (resolution of 4 cm^{-1}). Concerning the nanocomposite films, FT-IR analyses were carried out to infer the advance of the oxidation phenomena. Specifically, the samples were treated in an air oven at $T = 120$ °C, which is a temperature lower than the T_m of the polymer but high enough to accelerate the degradation processes. Then, FT-IR spectra were collected performing 16 scans between 4000 and 500 cm^{-1} on samples subjected to the above-mentioned thermo-oxidation treatment. The progress of the degradation was hence quantified by referring to the carbonyl (CI) and hydroxyl (HI) indices: the former represents the ratio between the integral of the carbonyl absorption region (1850–1600 cm^{-1}) and that of a reference peak at about 1370 cm^{-1}; the latter refers to the hydroxyl absorption region (3570–3150 cm^{-1}), which integral was normalized by the peak at 1370 cm^{-1}.

Thermogravimetric analysis (TGA) was carried out on the various kinds of CNTs using an Exstar TG/DTA Seiko 7200 instrument. The tests were performed at a heating rate of 10 °C/min from 30 to 750 °C under nitrogen flow. The reported results are the average of three independent measurements on batches of ~5 mg. The standard deviation was about 0.3% for each investigated sample.

The rheological tests were performed using a stress-controlled rheometer SR5 by Rheometrics Scientific in parallel plate geometry. The plate diameter was 25 mm. The complex viscosity (η^*) was measured performing frequency sweep tests at $T = 210$ °C from 10^{-1} to 10^2 rad/s considering a maximum strain of 2.0%. As proved by preliminary strain sweep experiments, such an amplitude is low enough to be in the linear viscoelastic regime.

Transmission Electron Microscopy (TEM) observations were performed at the Centro Grandi Apparecchiature – UninetLab, University of Palermo. The samples were mounted on the lacey carbon films on 300 mesh copper grids and then observed by JEOL JEM-2100 under accelerated voltage of 200 kV.

Alkyl-*f*-CNTs without and with immobilized VE, previously subjected to thermal treatment at either 50 or 210 °C for 5 min, were analyzed by micro-Raman spectroscopy at room temperature on a Bruker-Senterra micro-Raman equipped with a 532 nm diode laser excitation and 20 mW power. Non-confocal measurements were carried out in the range 4000–400 cm^{-1} with a spectral resolution between 9 and 15 cm^{-1}.

3. Results and discussion

3.1. *Identification of the physically immobilized VE on CNT surface*

The FT-IR spectra of pure VE and the various kinds of CNTs are shown in Fig. 2.

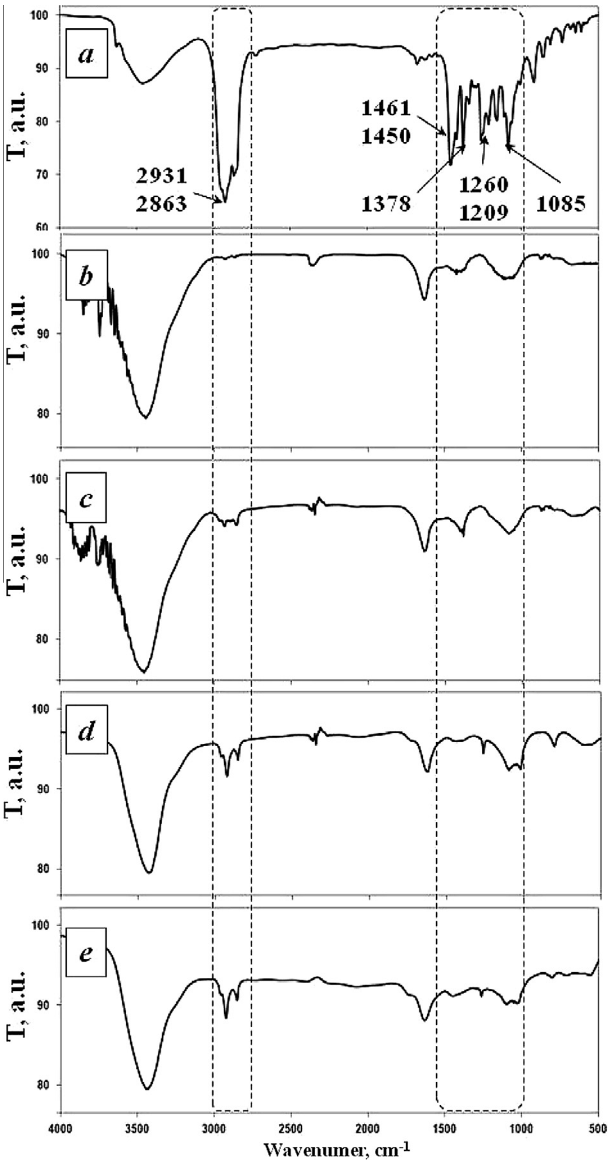

Fig. 2 – FT-IR spectra of (a) pure VE, (b) CNTs-COOH, (c) CNTs-COOH/VE, (d) alkyl-*f*-CNTs, (e) alkyl-*f*-CNTs/VE.

The main absorption bands of α-tocopherol are in the spectral range 1500–1000 cm^{-1} (see spectrum *a*). In particular, bands at 1450 cm^{-1} (phenyl skeletal bending), 1461 and 1378 cm^{-1} (methyl asymmetric and symmetric bending, respectively), 1264 and 1209 cm^{-1} (C–O stretching of the phenol group) and 1085 cm^{-1} (ether group) are noticed in agreement with the literature [15]. Since weak bands and/or small shoulders can be identified in the same spectral range (1500–1000 cm^{-1}) for the VE–free CNTs due to the presence of amorphous carbon [16], inferring the presence of VE molecules simply looking at the spectra *c* and *e* of the CNTs/VE is difficult. Nonetheless, the VE exhibits other specific absorption bands at about 2931 and 2863 cm^{-1} which are ascribed to the asymmetric and symmetric stretching of the methyl groups. These two specific bands are clearly detectable in the spectrum *c* of the CNTs-COOH/VE, revealing the presence of VE molecules in this sample. The same bands, however, can be also observed in the spectrum of the alkyl-*f*-CNTs. Therefore, univocally inferring the presence of adsorbed VE in the alkyl-*f*-CNT/VE sample only referring to the FT-IR results is difficult, and additional analyses are needed. More convincing proofs of the occurred functionalization come from the TGA analysis of the CNTs.

Apart from the weight loss around 100 °C, which is probably due to the loss a small amounts of residual water in all the CNT samples, both the CNT-COOH and alkyl-*f*-CNT samples decompose at temperature lower than the unmodified CNTs because of the volatilization of carboxyl groups and alkyl chains grafted on the CNT surface. The residuals at the end of the analysis were 98.2 wt.% and 97.3 wt.% for the CNT-COOH and alkyl-*f*-CNT sample, respectively, whereas a residual of 99.1 wt.% was found for the bare CNTs due to a partial decomposition of the bulk material. Concerning the CNTs/VE, both the CNTs-COOH/VE and alkyl-*f*-CNTs/VE exhibit more significant weight losses due to the VE volatilization. The latter begins at about 200 °C and finishes at about 400 °C (see inset of Fig. 3). The residues at the end of the analysis for CNTs-COOH/VE and alkyl-*f*-CNTs/VE are about 97.3 wt.% and 96.2 wt.% respectively, meaning that about 1 wt.% of VE remains immobilized on the CNTs at the end of our functionalization procedure.

3.2. *Stabilizing action of the CNTs/VE – Rheological analysis and thermo-oxidative resistance of the nanocomposites*

Rheology is particularly sensitive to molecular architecture of polymeric materials, being often used to infer the occurrence of degradation phenomena. The complex viscosity curves for the pure matrix and the nanocomposites are plotted in Fig. 4 as a function of frequency. The η^* values of all nanocomposites are higher than those of neat UHMWPE in the whole range of investigated frequency. The effect is particularly prominent for the CNT/VE samples at low frequency, where the melt state dynamics of larger portions of the polymer chains are probed. This suggests a beneficial effect the of VE molecules against the thermo-oxidation which may occur during the hot compaction processing step and in the course of rheological tests.

The stabilizing action of the CNTs/VE, however, plainly emerges by analyzing the time evolution of the FT-IR spectra in the course of the thermo-oxidation. The samples were treated in air at T = 120 °C to accelerate the oxidation process, which progress leads to the growth of both the carbonyl and hydroxyl indices. The CI refers to the signals in the range 1850–1600 cm^{-1}, which are due to the formation of different amount of carbonyl species and reflect the formation of acid (1715 cm^{-1}), ketones (1718 cm^{-1}), esters (1738 cm^{-1}) and lactones (1786 cm^{-1}). The HI is related to the presence of linked and free –OH groups deriving from the thermo-oxidation process. Indeed, the thermo-oxidation mechanism for UHMWPE mainly concerns the peroxide and hydroperoxide formation

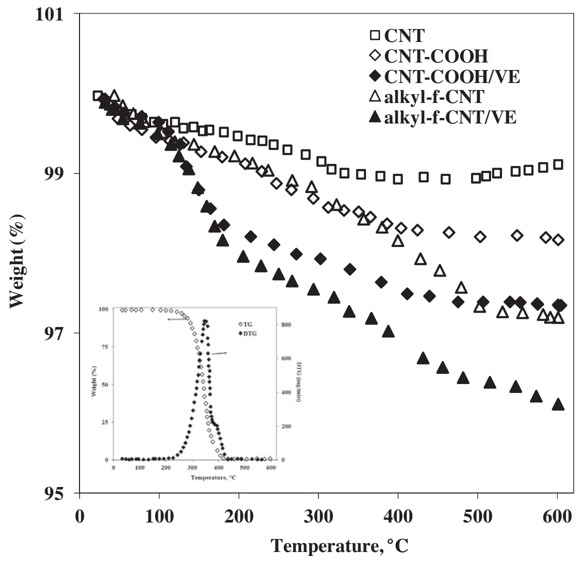

Fig. 3 – TGA analysis of unmodified CNTs, CNTs-COOH and alkyl-*f*-CNTs without and with immobilized VE. The inset shows TG and DTG curves of pure VE.

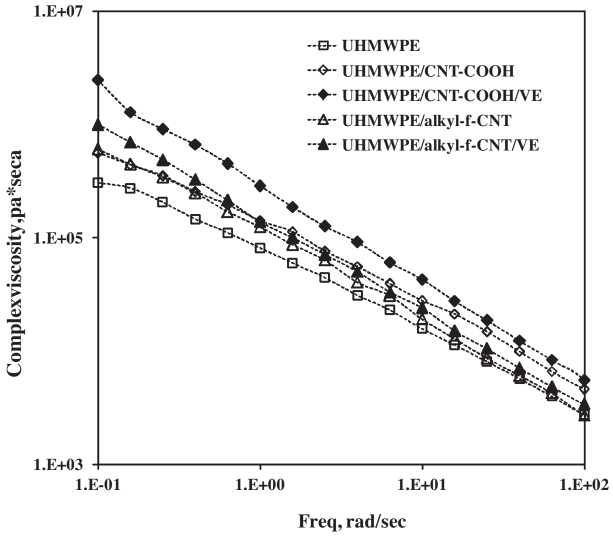

Fig. 4 – Complex viscosity of the UHMWPE-based nanocomposites. The complex viscosity of the neat polymer is reported for comparison.

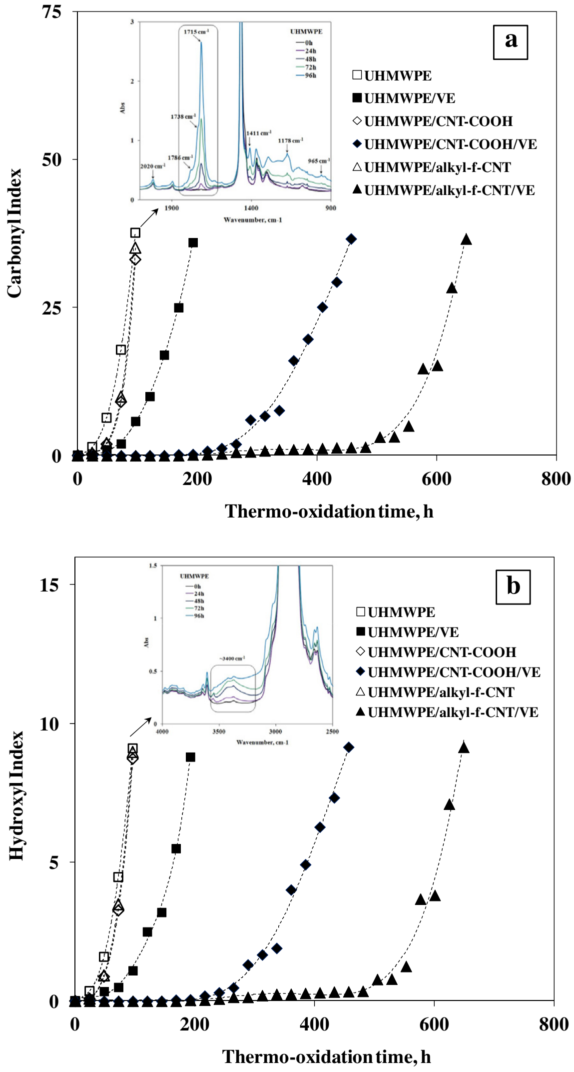

Fig. 5 – Carbonyl (a) and hydroxyl (b) indices as a function of the thermo-oxidation time. The insets show the FT-IR spectra of the UHMWPE in the range 2050–900 cm^{-1} (a) and 4000–2500 cm^{-1} (b) at different thermo-oxidation times. (A color version of this figure can be viewed online.)

and their later decomposition with formation of volatile products such as H_2O and, in lesser amounts, CO, CO_2 and H_2 [17].

The CI and HI of various polymer-based samples are shown in Fig. 5 as a function of the thermo-oxidation time. The degradation of the pure UHMWPE begins since the early stages of the thermo-oxidative treatment. It is worth noting that such chemical alterations are coupled with a drastic embrittlement of the material. A negligible increase of the thermo-oxidation resistance is attained upon addition of both CNTs-COOH and alkyl-*f*-CNTs. A radical scavenging action during processing and gamma irradiation [18,19] has been recently reported for CNT-filled polyethylene, while CNTs do not exert noticeable stabilizing action against photo-oxidation [20,21]. In contrast, a drastic increase of the thermo-oxidative resistance characterizes the samples containing the CNTs/VE. In particular, a fivefold increase of the induction time is noticed for the UHMWPE/CNT-COOH/VE with respect to UHMWPE, whereas a striking delay of the induction time of about ten time occurs for the UHMWPE/alkyl-*f*-CNT/VE sample. We also notice that the samples containing the CNTs/VE exhibit a slower grow rate of both CI and HI after the induction period. Such noteworthy results cannot be simply explained by invoking the antioxidant feature of the VE molecules. As shown in Fig. 5, in fact, even adding 0.1 wt.% of VE not immobilized on the CNTs, that is to say an amount of antioxidant much higher than that actually present in our nanocomposite samples (see Fig. 3), the improvement of the of the thermo-oxidation resistance is much less important. The possible origins of the synergy between VE and CNTs are discussed in the next Section.

3.3. *Discussion about the stabilization mechanism*

The origin of the results shown in Fig. 5 has to be sought in the specific interactions which establish between the VE molecules and the CNTs. We believe that the VE may induce structural defects on the surface of the CNTs, which act as acceptor-like localized states conferring free-radical scavenging activity to the nanoparticles. Recent experimental [22,23] and theoretical [24] studies corroborate this hypothesis.

In our specific case, two different mechanisms for the formation of CNT surface defects can be proposed. The first one is based on the reductant feature of α-tocopherol. VE is able to reduce some of the oxygen-containing functional groups located onto the CNT surface. Removing oxygen-containing groups can leave carbon-centered defects in the carbonaceous surfaces. As reported in literature for graphene oxide [25–26], its reduction to graphene envisages the formation of surface defects as byproducts. The mechanisms for these reactions are well documented for reducing agents having chemical structure similar to α-tocopherol, such as ascorbic acid [27], gallic acid [28] and polyphenols [29].

A second plausible mechanism for the formation of CNT surface defects involves the carbon atoms on the outer surface of the CNTs. A potentially strong interaction between ascorbic acid (vitamin C) and nicotinamide (vitamin B3) radicals and carbon atoms onto the CNT has been recently predicted by De Menezes *et al.* via *ab initio* theoretical calculations based on the density functional theory [30,31]. The radicals coming from vitamin C and B3 induce a degeneracy of the electronic bands of the CNTs breaking their mirror symmetry. As a consequence, some carbon atoms of the CNT outer surface change the hybridization from sp^2 to sp^3-like (see Fig. 6(a)). The same hybridisation changes take place when the carbon atoms are covalently linked to functional groups or in presence of lattice defects onto the CNT surface. As a result, the damaged CNTs behave as free-radical scavengers.

Strong interactions similar to those mentioned above could establish between the VE molecules and CNTs. More specifically, the VE could convert by thermal energy into different radical intermediates, such as O-centered tocopheroxyl radical, C-centered α,β-insaturated ketons and/or tocoquinone [9,10]. Such species interact with the CNTs surface, changing the hybridization of the outer carbon atoms as schematically shown in Fig. 6(b). It is important to notice that such kinds of interaction are favored if the radicals are close to the

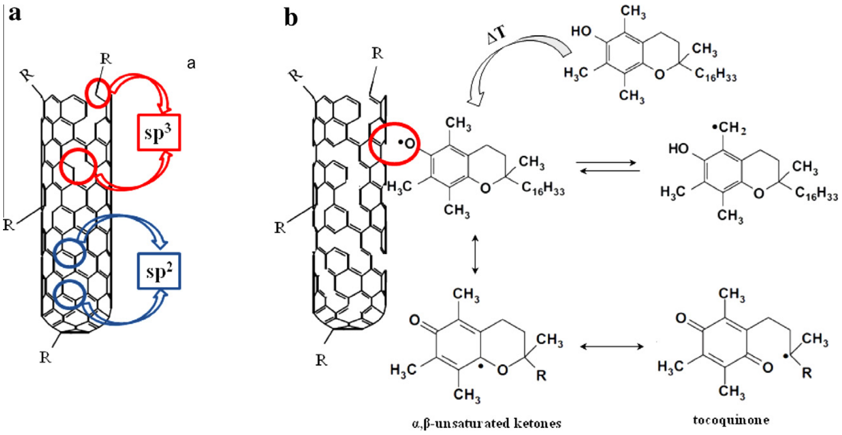

Fig. 6 – Schematic representation of the hybridization of the carbon atoms onto the CNT surface without and with surface defects (a), and possible interactions between a CNTs and VE radical intermediates (b). (A color version of this figure can be viewed online.)

CNT surface, which satisfy the assumptions of the *ab initio* theoretical calculations.

Based on the previous considerations, the excellent thermo-oxidation resistance of our samples containing CNTs/VE is ultimately ascribable to the VE-induced defects on the surface of the CNTs. The presence of the latter can be assessed through Raman spectroscopy. In particular, the ratio between the signal intensities of the disordered-induced D-band at ~1340 cm^{-1} (I_D) and tangential G-band at ~1580 cm^{-1} (I_G) is related to structural defects in CNTs [32,33]. The Raman spectra of the VE-free and VE containing alkyl-*f*-CNTs are compared in Fig. 7 before and after thermal treatment for 5 min at 210 °C; the latter simulates the thermal history experienced by the CNTs during the preparation of the nanocomposites.

The I_D/I_G ratio of the alkyl-*f*-CNTs remains unchanged upon thermal treatment, whereas it increases from 0.76 to 0.82 in the presence of immobilized VE. It is hence confirmed that the latter could promote defects on the walls of the CNTs at high temperature, i.e. during processing and/or the thermo-oxidation protocol. Moreover, the structure of alkyl-*f*-CNT/VE sample after thermal treatment appears more damaged and this finding can be related to the obtained Raman result, suggesting that the structural changes are due to larger amount of surface defects.

Finally, we try to explain why the VE is more effective for the alkyl-*f*-CNTs/VE than for the CNTs-COOH. First, as emerged from the TGA analyses, the long alkyl functional groups could be able to entrap a larger amount of VE

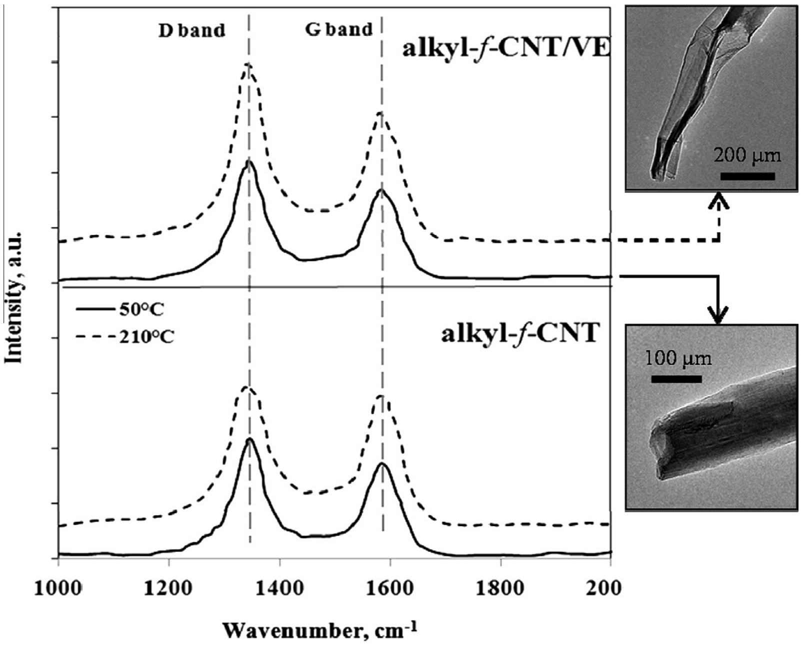

Fig. 7 – Raman spectra of the alkyl-*f*-CNTs with and without immobilized VE molecules after thermal treatment at 50 and 210 °C for 5 min. Representative TEM micrographs of a alkyl-*f*-CNTs/VE before and after thermal treatment are shown as well.

molecules. Additionally, the alkyl chains could limit the migration of the VE molecules towards the matrix. Remaining closer to the CNT surface, the VE molecules could establish stronger interactions with the CNTs, thus inducing a more intensive radical scavenging action compared to the less interacting CNTs-COOH/VE samples.

4. Conclusions

Antioxidant VE molecules have been physically immobilized onto the outer surface of multi-walled CNTs bearing covalently linked carboxylic acid and long-chain alkyl ester functionalizing groups. The resulting CNTs/VE have been used to prepare thermally-stable UHMWPE-based nanocomposites. The effective immobilization of the VE molecules has been confirmed by spectroscopic and thermal analyses. The nanocomposites containing the CNTs/VE exhibit surprisingly high resistance to oxidation. In particular, a ten-fold increase of the induction time has been noticed for the UHMWPE/alkyl-*f*-CNT/VE sample with respect to the unfilled polymer. Rather than to the inherent antioxidant feature of the immobilized molecules, such a result is proposed to originate from a radical scavenging activity induced by the VE molecules, which promote the formation of structural defects on the surface of the CNTs. Two plausible mechanisms have been proposed to explain the VE-induced damage of the CNT surface: the first one envisages the interactions between the VE and the oxygen-containing functional groups of the CNTs; the second refers to the direct interactions with the carbon atoms of the CNTs. The presence of structural defect has been demonstrated through Raman spectroscopy. Irrespective of their origin, the surface defects represent acceptor-like localized states, being ultimately responsible for the excellent antioxidant feature of our nanocomposites.

Acknowledgments

This work has been financially supported by Ministry of University and Research in Italy (MIUR), FIRB2010 – Futuro in Ricerca, Project title: “GREENER – Towards multifunctional, efficient, safe and stable “green” bio-plastics based nanocomposites of technological interest via the immobilization of functionalized nanoparticles and stabilizing molecules” (cod: RBFR10DCS7).

REFERENCES

[1] Spitalskya Z, Tasisb D, Papagelisb K, Galiotis C. Carbon nanotube–polymer composites: chemistry, processing, mechanical and electrical properties. Prog Polym Sci 2010;35(3):357–401.

[2] Coleman JN, Khan U, Blau WJ, Gun’ko YK. Small but strong: a review of the mechanical properties of carbon nanotube–polymer composites. Carbon 2006;44(9):1624–52.

[3] Peigney A, Laurent C, Flahaut E, Bacsa RR, Rousset A. Specific surface area of carbon nanotubes and bundles of carbon nanotubes. Carbon 2001;39(4):507–14.

[4] Dintcheva NTz, Arrigo R, Nasillo G, Caponetti E, La Mantia FP. On the role of extensional flow in morphology and property modifications of MWCNT/polyamide-based fibers. Macromol Mater Eng 2011;296(7):645–57.

[5] Mawhinney DB, Naumenko V, Kuznetsova A, Yates Jr JT, Liu J, Smalley RE. Surface defect site density on single walled carbon nanotubes by titration. Chem Phys Lett 2000;324(1–3): 213–6.

[6] Yang M, Gao Y, Li H, Adronov A. Functionalization of multiwalled carbon nanotubes with polyamide 6 by anionic ring-opening polymerization. Carbon 2007;45(12):2327–33.

[7] Nativ-Roth E, Shvartzman-Cohen R, Bounioux C, Florent M, Zhang D, Szleifer I, et al. Physical adsorption of block copolymers to SWNT and MWNT: a nonwraping mechanism. Macromolecules 2007;40(10):3676–85.

[8] Campidelli S, Ballesteros B, Filoramo A, Dıaz DD, Torre G, Torres T, et al. Facile decoration of functionalized single-wall carbon nanotubes with phthalocyanines via click chemistry. J Am Chem Soc 2008;130(34):11503–9.

[9] Al-Malaika S, Ashley H, Issenhuth S. The antioxidant role of α -tocopherol in polymers. I. The nature of transformation products of α -tocopherol formed during melt processing of LDPE. J Polym Sci Part A Polym Chem 1994;32(16):3099–113.

[10] Al-Malaika S, Goodwin C, Issenhuth S, Burdick D. The antioxidant role of α -tocopherol in polymers II. Melt stabilising effect in polypropylene. Polym Degrad Stab 1999;64(1):145–6.

[11] Gonçalves CMB, Tomé LC, Coutinho JAP, Marrucho IM. Addition of α-tocopherol on poly(lactic acid): thermal, mechanical, and sorption properties. J Appl Polym Sci 2011;119(4):2468–75.

[12] Oral E, Muratoglu OK. Vitamin E diffused, highly crosslinked UHMWPE: a review. Int Orthop 2011;35(2):215–23.

[13] Bracco P, Oral E. Vitamin E-stabilized UHMWPE for total joint implants: a review. Clinical Orthop Relat Res 2011;469(8):2286–93.

[14] Fu J, Shen J, Gao G, Xu Y, Hou R, Cong Y, et al. Natural polyphenol-stabilized highly crosslinked UHMWPE with high mechanical properties and low wear for joint implants. J Mater Chem B 2013;1(37):4727–35.

[15] Che Man YB, Ammawath W, Mirghani MES. Determining a-tocopherol in refined bleached and deodorized palm olein by Fourier transform infrared spectroscopy. Food Chem 2005;90(1–2):323–7.

[16] Carroccio SC, Curcuruto G, Dintcheva NTz, Gambarotti C, Coiai S, Filippone G. Using matrix-assisted laser desorption/ionization time-of-flight mass spectrometry for the characterization of functionalized carbon nanotubes. Rapid Commun Mass Spectrom 2013;27(12):1359–66.

[17] Costa L, Luda MP, Trossarelli L. Ultra high molecular weight polyethylene—II. Thermal- and photo-oxidation. Polym Degrad Stab 1997;58(1–2):41–54.

[18] Castell P, Martinez-Morlanes MJ, Alonso PJ, Martinez MT, Puertolas JA. A novel approach to the chemical stabilization of gamma-irradiated ultrahigh molecular weight polyethylene using arc-discharge multi-walled carbon nanotubes. J Mater Sci 2013;48(19):6549–57.

[19] Martinez-Morlanes MJ, Castell P, Alonso PJ, Martinez MT, Puertolas JA. Multi-walled carbon nanotubes acting as free radical scavengers in gamma-irradiated ultrahigh molecular weight polyethylene composites. Carbon 2012; 50(7):2442–52.

[20] Dintcheva NTz, La Mantia FP, Malatesta V. Photo-oxidation behaviour of polyethylene/multi-wall carbon nanotube composite films. Polym Degrad Stab 2009;94(2):162–70.

[21] Morlat-Therias S, Fanton E, Gardette JL, Peeterbroeck S, Alexandre M, Dubois P. Polymer/carbon nanotube nanocomposites: Influence of carbon nanotubes on EVA photodegradation. Polym Degrad Stab 2007;92(10):1873–82.

[22] Watts PCP, Fearon PK, Hsu WK, Billingham NC, Kroto HW, Walton DRM. Carbon nanotubes as polymer antioxidant. J Mater Chem 2003;13(3):491–5.

[23] Shi X, Jiang B, Wang J, Yang Y. Influence of wall number and surface functionalization of carbon nanotubes on their antioxidant behavior in high density polyethylene. Carbon 2012;50(3):1005–13.

[24] Galano A, Francisco-Marquez M, Martinez A. Influence of point defects on the free-radical scavenging capability of single-walled carbon nanotubes. J Phys Chem C 2010;114(18):8302–8.

[25] Pei S, Cheng H-M. The reduction of the graphene oxide. Carbon 2012;50(9):3210–28.

[26] Chua CK, Pumera M. Chemical reduction of graphene oxide: a synthetic chemistry viewpoint. Chem Soc Rev 2014;43(1):291–312.

[27] Gao J, Liu F, Liu Y, Ma N, Wang Zh, Zhang X. Environment-friendly method to produce graphene that employs vitamin c and amino acid. Chem Mater 2010;22(7):2213–8.

[28] Li J, Xiao G, Chen C, Lia R, Yana D. Superior dispersions of reduced graphene oxide synthesized by using gallic acid as a reductant and stabilizer. J Mater Chem A 2013;1:1481–7.

[29] Liao R, Tang Z, Lei Y, Guo B. Polyphenol-reduced graphene oxide: mechanism and derivatization. J Phys Chem C 2011;115(42):20740–6.

[30] De Menezes VM, Fagan SB, Zanella I, Mota R. Carbon nanotubes interacting with vitamins: first principles calculations. Microelectr J 2009;40(4–5):877–9.

[31] Cadore AR, Zanella I, de Menezes VM, Rossato J, Mota R, Fagan SB. Metal-doped carbon nanotubes interacting with vitamin C. Phys Chem Chem Phys 2012;14(48):16737–44.

[32] Qian WZ, Liu T, Wei F, Yuan HY. Quantitative Raman characterization of the mixed samples of the single and multi-wall carbon nanotubes. Carbon 2003;41(9):1851–4.

[33] Sinha AK, Bhalerao GM, Sathe V. Defect-dependent annealing behavior of multi-walled carbon nanotubes. Physica E 2008;41(1):54–9.